J. Micromech. Microeng. **17** (2007) S237–S242 doi:10.1088/0960-1317/17/9/S05

A MEMS-based reformed methanol fuel cell for portable power

J D Morse[1], R S Upadhye[1], R T Graff[1], C Spadaccini[1], H G Park[1] and E K Hart[2]

[1] Lawrence Livermore National Laboratory, Center for Meso, Micro, and Nano Technology, 7000 East Ave, Livermore, CA 94550, USA
[2] Department of Materials Science, Stanford University, Stanford, CA 94305, USA

E-mail: morse3@llnl.gov

Received 14 February 2007, in final form 15 April 2007
Published 31 August 2007
Online at stacks.iop.org/JMM/17/S237

Abstract
A reformed methanol fuel cell system is described. The use of a microfluidic fuel processor enables component scaling and integration sufficient to achieve power sources in the 2–10 W regime that are competitive in size and energy density in comparison to alternative power sources. While carbon monoxide tolerance of proton conducting membranes has typically limited the performance of reformed methanol fuel cells, phosphoric-acid-doped polybenzimidazole (PBI) membranes have been tested that exhibit no degradation for carbon monoxide >2% mole fraction. Further benefits of the PBI membrane include operating temperature of 150–200 °C, and no need for water to assist protonic conduction. As a result, a chemically and thermally robust fuel cell power source is realized. Results of methanol steam reforming and catalytic combustor heating elements formed in a silicon MEMS platform, and PBI membrane performance with reformate fuel feed will be discussed.

1. Introduction

Micro-fuel cells have received considerable attention over the past decade as a primary solution to the increased demands on portable power sources [1–3]. Fuel cells have the key advantage that the energy is stored in chemical form in the fuel; therefore if the energy conversion platform (i.e., the fuel cell stack) can be made sufficiently small, and the fuel can be provided in easy to handle high concentration cartridges, then a fuel cell will provide extended time between recharge for comparably sized rechargeable batteries. Furthermore, recharging is instantaneous by replacement of the fuel cartridge. These latter points have become the driving factor for the range of micro-fuel cell technologies that are being developed today. The research and development path towards realizing a miniature fuel cell power source has explored a range of system implementations utilizing hydrocarbon or hydrogen containing fuels [4–6], several variations for the ion conducting media [7–9], and incorporating varying degrees of microfabrication [10–13].

MEMS micromachining techniques offer a method to monolithically integrate key components of the fuel cell stack, including microfluidic flow field, gas diffusion layer, current collectors, electrodes and possibly the membrane electrode assembly through a continuous fabrication sequence [11]. Using similar MEMS configuration, both DMFC and hydrogen fuel cells have been demonstrated using either an MEA compressed between two silicon substrates, or a membrane electrode assembly grafted to the metallized silicon surface using a solution of Nafion and carbon black to provide good contact between the current collector and electrolyte interface. Other modifications of this have been demonstrated with varied results. Lee *et al* [7] reported arrays of hydrogen–air PEM fuel cells formed on silicon substrates wherein a reconfigurable cathode electrode enabled scaling of either current or voltage. An additional configuration reported has been to form the porous silicon or silicon dioxide catalyst/electrode support on the same side of the silicon wafer using a sacrificial surface micromachining approach [13, 14]. For either configuration a reduction in component count is achieved along with decrease of critical features for flow field channels. One of the

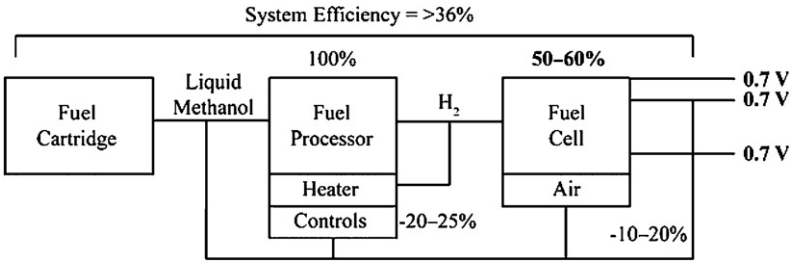

Figure 1. Schematic diagram of RMFC.

limiting factors of MEMS fuel cells seems to be low power density compared to other approaches, possibly due to the limited compression that can be applied to the fragile silicon substrates.

Scaling of fuel cells for portable power sources in the 2–10 W regime requires new methodologies and design schemes to compete with primary and rechargeable battery technologies. A key focus for portable fuel cells has been the use of hydrocarbon fuels as a result of the high volumetric energy density. Methanol has gained the most attention since it can be easily stored in liquid form, with catalytic reactions releasing the hydrogen occurring at relatively low temperatures. While the prospect of utilizing methanol directly at the fuel cell anode is encouraging, direct methanol fuel cells (DMFCs) are limited to low concentrations of methanol (1–2 M) delivered to the anode in order to reduce the effects of methanol crossover of the Nafion membrane [5]. This necessitates a complex water management system for DMFCs that effectively reduces the energy density of the fuel cell power source. Furthermore, the low activity of the methanol–water kinetics at the anode limits the power density that can be achieved for these systems.

This paper describes the fabrication and performance of a MEMS-based reformed methanol fuel cell (RMFC) system. Reformed methanol fuel cells provide an option for micro-fuel cell power sources whereby high concentration methanol–water fuel mixtures can be utilized, providing a higher energy and power density system. Limitations for RMFC systems include thermal management of high temperature components, and tolerance of fuel cell anode catalyst to residual carbon monoxide (CO) in the reformate fuel feed. Nafion-based membranes are limited to low temperature ($<100\ ^\circ$C) operation due to the membrane drying out, which effectively degrades the proton conductivity of the membrane. At these temperatures, CO adsorbs to the anode catalyst, resulting in a long-term poisoning effect that is difficult to reverse. High temperature ($>120\ ^\circ$C) phosphoric-acid-doped polybenzimidazole (PBI) membranes offer increased CO tolerance [15]. Utilizing PBI membranes, results for a MEMS-based RMFC system are presented below, demonstrating the unique aspects and performance of a microfluidic fuel processor formed in silicon having both methanol steam reforming and catalytic combustion heater in a monolithic design.

2. Reformed methanol fuel cell

Steam reforming of methanol is an endothermic catalytic process described by the reaction:

$$CH_3OH + H_2O \rightarrow 3H_2 + CO_2 \quad \Delta H = 126 \text{ kJ mol}^{-1}. \quad (1)$$

From (1), ΔH is the higher heating value of the reactants. For a $CuZnO/Al_2O_3$ catalyst [16], reaction (1) occurs in the 250–300 °C range producing a hydrogen rich fuel feed to the fuel cell anode with an approximate composition of 75% H_2, 24% CO_2 and <1% CO. The RMFC system diagram is illustrated in figure 1. The heat needed for the steam reforming is supplied by either a resistive or catalytic heater, with the latter being more convenient since the fuel supply and any unutilized fuel from the fuel cell anode will drive the catalytic reactions described by

$$CH_3OH + 3/2\,O_2 \rightarrow 2H_2O + CO_2 \quad (2)$$

and

$$H_2 + 1/2O_2 \rightarrow H_2O. \quad (3)$$

From (3) above, $\Delta H = -243$ kJ mol^{-1} is the exothermic energy produced by the reaction. Theoretically, 1 mole of methanol generates 3 moles of hydrogen and the combustion of 0.5 mole of hydrogen (17% of generated hydrogen) can provide the higher heating value (i.e., lower heating value plus latent heat) of the methanol steam reforming process. Due to both the thermal loss to ambient through an insulated package and enthalpy retained in the outflow, the required hydrogen flow in the micro-combustor will be higher.

Therefore, the above exothermic reactions will provide heat to drive the endothermic steam reforming process. RMFC systems enable the use of high concentration methanol fuel that only has to be diluted to approximately 1:1 steam-to-methanol ratio for effective reforming. This provides a hydrogen rich fuel feed for the fuel cell, and high power density proton exchange membrane (PEM) fuel cells can be used to justify the added complexity of the thermal components for fuel processing. For the reformed methanol fuel cell, the anode reaction is described by

$$2H_2 \rightarrow 4H^+ + 4e^- \quad (4)$$

and the cathode reaction is described as

$$O_2 + 4H^+ + 4e^- \rightarrow 2H_2O. \quad (5)$$

The nominal anode and cathode catalyst for the reactions described above is platinum, and oxygen is delivered to the cathode from ambient air. From the schematic shown in figure 1, the fuel utilization at the anode of the fuel cell is on the order of 80% for appropriately designed flow fields, thereby providing sufficient hydrogen from the anode effluent fed back into the catalytic combustor to generate the necessary heat of reaction required for the methanol steam reforming.

As previously mentioned, a key issue with this approach is that the small quantity (<1%) of CO present in the fuel feed

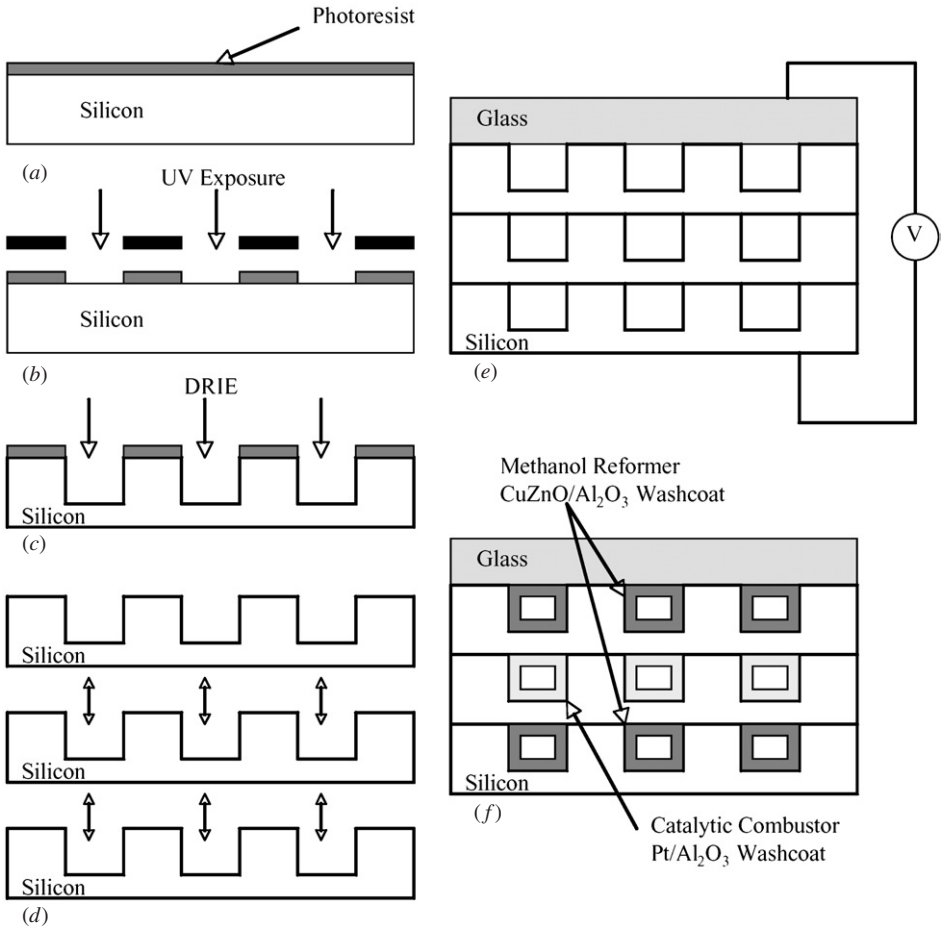

Figure 2. Schematic cross section of microfluidic fuel processor fabrication sequence: (*a*) coat silicon with thick photoresist, (*b*) photolithographic patterning, (*c*) deep reactive ion etch of silicon forming microchannels, (*d*) fusion bonding of silicon wafers, (*e*) anodic bond of glass cover to silicon stack and (*f*) wash coating of the $CuZnO/Al_2O_3$ reformer catalyst and Pt/Al_2O_3 combustor catalyst on microchannel sidewalls for respective chambers.

from the reaction described by (1) is sufficient to poison the anode catalyst at typical operating temperatures for Nafion-based fuel cells (25–80 °C). Various approaches have been investigated including preferential oxidation, water–gas shift reactors or absorbers to remove the CO from the fuel feed [17]. These approaches have had limited success for low temperature (<100 °C) PEM fuel cells as CO concentrations present in the fuel feed at the 50–100 parts per million range are sufficient to degrade anode catalyst performance.

In order to optimize RMFC system operation, a membrane electrode assembly (MEA) that operates at >150 °C is desired such that any CO present in the fuel feed will rapidly desorb from the anode catalyst, resulting in limited degradation. The use of phosphoric-acid-doped polybenzimidizole (PBI) membranes [15] enables an MEA technology that performs at >150 °C has sufficient proton conductivity to be competitive with Nafion, and has the benefit of not requiring any humidification for efficient operation. The drawback is the membranes do not operate well at temperatures <140 °C, so startup requires that the MEA and fuel cell stack be brought up to temperature before significant power is delivered. To provide thermal integration, rapid startup, and microminiaturization of the RMFC fuel cell power source, MEMS-based methanol steam reformers have been demonstrated [18, 19]. The design and performance of a microfluidic steam reformer integrated monolithically with a catalytic combustor is described, along with the nominal performance of the RMFC system for a 3–5 W power source.

3. Microfluidic fuel processor

3.1. Fuel processor fabrication

MEMS fabrication techniques provide the means to integrate a steam reformer and catalytic combustor in a single monolithic design. The fuel processor design utilizes deep reactive ion etching (DRIE) to form high aspect ratio microchannel arrays. This specific design incorporates a wraparound reformer surrounding the catalytic microcombustor. The catalyst bed for both reformer and combustor is formed using DRIE to etch microchannels of 200 μm diameter, 850 μm depth and 250 μm center-to-center spacing. The microfabrication sequence is illustrated in figure 2. The substrate used is a double side polished, 20 Ω cm, boron-doped, 100 mm diameter silicon wafer with a nominal thickness of 1 mm. A layer of thick photoresist is coated onto the topside of the silicon wafer by spinning at a rate of 1000 rpm for 30 s. The photoresist is then soft baked at 90 °C for 20 min.

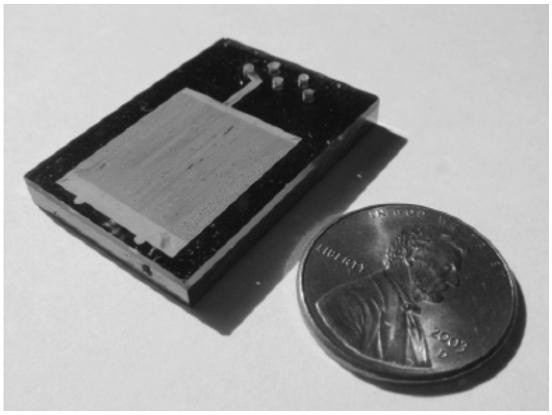

Figure 3. Integrated fuel processor chip.

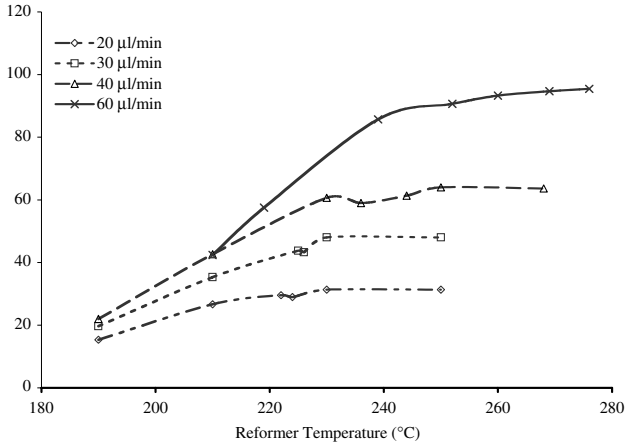

Figure 4. Reformate output flow rate as a function of temperature for several methanol–water fuel inlet flow rates. Complete conversion (100%) is achieved at reformer outlet flow rates of 16, 32, 48 and 96 ml min^{-1} for inlet fuel flow rates of 20, 30, 40 and 60 μl min^{-1}, respectively.

For this particular fuel processor design, channel depths of 850 μm are required; therefore photoresist thickness on the order of 14 μm is used as a mask for the silicon deep reactive ion etch process, which typically exhibits an etch selectivity of 70–100:1 for the etch parameters used. The resist is exposed and developed to form the microchannel patterns for the fuel processor device. Microchannels were etched to an approximate depth of 850 μm using the Bosch process, resulting in reasonably smooth, vertical sidewalls. Through wafer vias are formed using the same procedure, aligning patterns to be etched from the backside of the wafer to select patterns etched on the top side in the step described above. In this manner, vias are formed providing inlet and outlet flow for different reactor chambers, as well as microfluidic interconnections between different layers of the fuel processor.

The silicon wafer is then cleaned and prepared for wafer bonding. In this fuel processor design, three silicon wafers containing microchannel arrays were used. The wafers were carefully aligned and fusion bonded at 1200 °C for 2 h. The center wafer is the catalytic combustor chamber, with the outer wafers used for the methanol reformer chamber which wraps around the combustor to effectively transfer the heat necessary to sustain the reforming reactions. The top silicon wafer was capped with a glass wafer that had vias formed by laser drilling to provide inlet and outlet access to the reformer and combustion chambers. The glass was carefully aligned to the silicon stack, and then anodically bonded at a temperature of 450 for 1 h. A slow temperature ramping was used during the anodic bond step in order to avoid effects of thermal stresses on the glass to silicon interface, which can result in cracking or disbonding. The schematic of the fully bonded structure is illustrated in figure 2(f). The wafer was subsequently diced up using a diamond saw, after which the catalyst is applied to each chamber using a wash coating process. For the reformer, a $CuZnO/Al_2O_3$ (30 wt% Cu) composition is used, and for the catalytic combustor a Pt/Al_2O_3 (5 wt% Pt) composition is applied. Typical quantities for each catalyst bed are 78 mg of $CuZnO/Al_2O_3$ in the steam reforming section, and 38 mg of Pt/Al_2O_3 in the combustor section. Figure 3 illustrates the integrated fuel processor chip.

3.2. Fuel processor characterization

Methanol steam reforming was characterized using a CH_3OH:H_2O (1:1.1) inlet flow controlled by a syringe pump. Fluidic connection to the fuel processor was achieved using 0.04″ internal diameter stainless steel tubing using a compression fitting with high temperature silicone o-rings. Initial testing to characterize catalyst performance was conducted using resistive heaters attached to one surface of the integrated silicon fuel processor. The fuel processor chip was thermally insulated using a 0.5″ thick layer of Kapton foam that was wrapped around the chip and held using Kapton tape. A type-K thermocouple was attached to the surface of the silicon fuel processor to accurately monitor the temperature of the reformer. This temperature is assumed to be within 5 °C of the catalyst bed temperature due to the high thermal conductivity of silicon and the high surface to volume ratio of the fuel processor. The reformer catalyst was characterized as a function of temperature and for different flow rates. The results are illustrated in figure 4.

From the results in figure 4, the per cent conversion of fuel feed to products is the ratio of the outlet flow at a given temperature to the 100% conversion outlet flow, which is the point where each curve saturates, remaining constant with further temperature increases. Higher inlet fuel flow would shift the point where outlet flow saturates (i.e., 100% conversion) higher temperatures for the same quantity of catalyst. Thus, for specific system designs, the appropriate operating temperature and flow rates can be chosen. The catalytic combustor design provides efficient conversion of unutilized fuel from the fuel cell anode to heat the steam reformer through the exothermic reactions described by (2) and (3). Directly coupling the combustion chamber to the reformer chamber through the integrated MEMS design enables rapid heat transfer and spreading to the high surface area reformer catalyst bed. Additionally, for the fuel cell operation, it is easier to design flow fields that utilize 75–80% of the anode fuel feed, compared to 90–100% utilization. The catalytic combustor was tested using both hydrogen and pure methanol

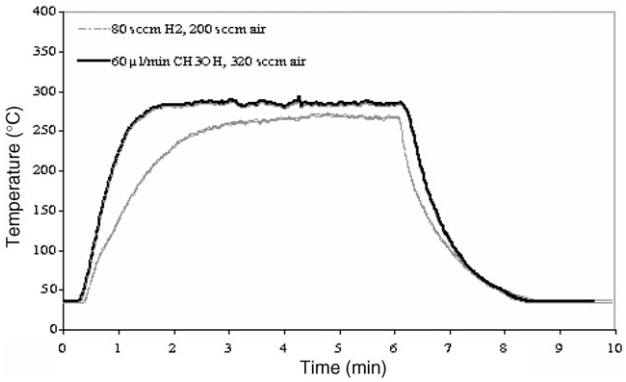

Figure 5. Microchannel combustor temperature as a function of time for both methanol and hydrogen fuel.

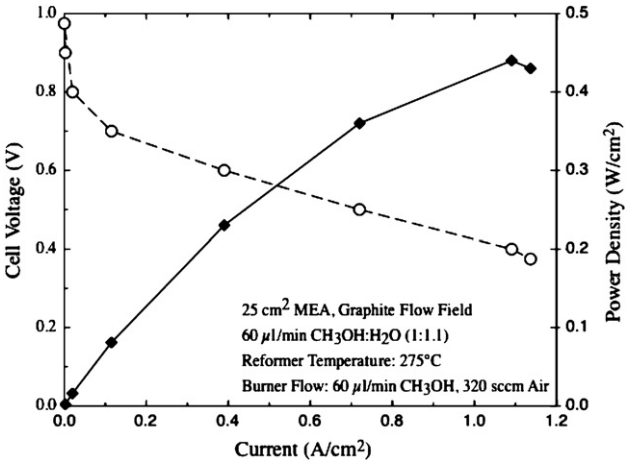

Figure 6. Performance of a PBI membrane fuel cell using the methanol–water reformate fuel.

as fuels. By volume, a fuel/oxygen ratio between 1 and 1.2 is used for optimal reactions. In the case of methanol fuel, the air feed flows over the methanol inlet causing the fuel to evaporate and flow into the combustor chamber in vapor phase. Figure 5 shows the combustor thermal ramp-up from room temperature.

In operation, the fuel processor would be ramped up to temperature prior to any fuel flow into the steam-reforming catalyst bed. Similarly in turning off the fuel processor, the preferred method would be stopping the methanol–water mixture flow to the steam reforming chamber enabling the catalyst to dry out, and then ramping down the combustor temperature by decreasing the fuel flow. In practice, these operations can be readily achieved using integrated micropumps and microvalves.

4. Fuel cell performance

As discussed previously, CO poisoning of the fuel cell anode catalyst is of key concern for reformate-fed fuel cells. Previous performance with Nafion PEM fuel cells has exhibited rapid degradation and long-term stability at low temperatures (<100 °C) using reformate feeds having CO in the >0.01% range. Recent improvements in phosphoric-acid-doped PBI membranes make this a viable candidate for RMFC systems. Polybenzimidazole (PBI) membranes are cast from solutions of PBI/trifluoacetyl/H_3PO_4 with optimized acid doping levels [15]. While the main benefit of phosphoric-acid-doped PBI membranes is the high temperature (120–200 °C) operation enabling high anode tolerance to significant quantities of CO (>1%), PBI membranes have additional qualities of good proton conductivity, low gas permeability, performance almost independent of relative humidity and good mechanical stability. Figure 6 illustrates the performance of a phosphoric-acid-doped, PBI membrane fuel cell utilizing reformate fuel produced from a microfluidic fuel processor. The fuel cell electrode area is 5 cm × 5 cm, with a flow field formed in graphite plates. The fuel flow into the fuel processor is 60 μl min^{-1}, providing a nominal reformate feed to the fuel cell of ∼190 ml min^{-1}. The cathode air flow was maintained at 900 sccm, with an estimated volumetric oxygen to fuel ratio of 2.5 for optimal fuel cell performance. The fuel cell was operated at 180 °C, and in this case a hot plate and thermocouple feedback loop was used to maintain the temperature. The catalytic combustor was heated using a separate methanol feed of 60 ml min^{-1} controlled by a syringe pump, mixed with 320 sccm air. Overall, the fuel cell operation was stable for several hours over which testing occurred. The PBI membrane exhibited a nominal power density of 230 mW cm^{-2} at a cell potential of 0.6 V (57% efficient), with the possibility of further improvements through optimization of membrane electrode assembly compression by the graphite plates.

A key remaining issue is the inability of the PBI membrane to operate at room temperature; therefore some fraction of system energy must be utilized to heat up and maintain the fuel cell stack temperature during operation. By appropriate stack and system design, the steady state operating temperature can be maintained by the fuel cell losses, i.e., for a 57% efficient fuel cell, 43% of the power goes to waste heat. To address startup operation, the catalytic combustor provides sufficient means of generating the necessary heat, as well as the ability for a cold start, so long as the thermal mass of the fuel cell component remains small enough. One method that has been explored is the use of MEMS-based fuel cells whereby the typical components of a fuel cell are formed in a silicon substrate via micromachining approaches. The benefit of this approach includes reduction of size and mass, good thermal conductivity through silicon, and components that can be integrated in a monolithic fashion. The latter includes formation of flow fields, gas diffusion layer, electrodes and even membrane electrode assemblies through a continuous fabrication process flow. Figure 7 illustrates an example of a MEMS-based fuel cell platform. In this example, the flow field, gas diffusion layer and current collector electrode have been formed on a silicon chip using DRIE and thin film sputtering processes. From the figure, the flow field channels are evident. The channel widths are 400 μm and 400 μm depth. The flow field is laid out to provide a constant pressure drop from inlet to outlet.

The gas diffusion layer consists of arrays of micropores etched in the silicon connecting the bottom of the flow field channels to the electrode layer as shown in figure 8. The pores were formed using DRIE techniques, with features of 4 μm

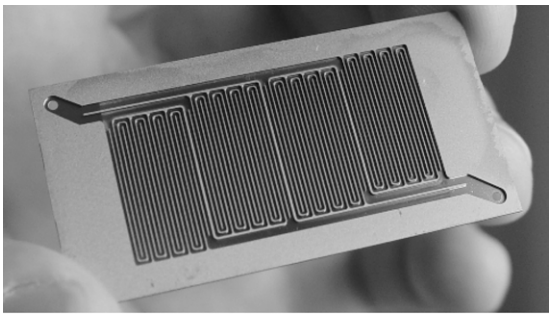

Figure 7. Flow field formed in silicon substrate using DRIE.

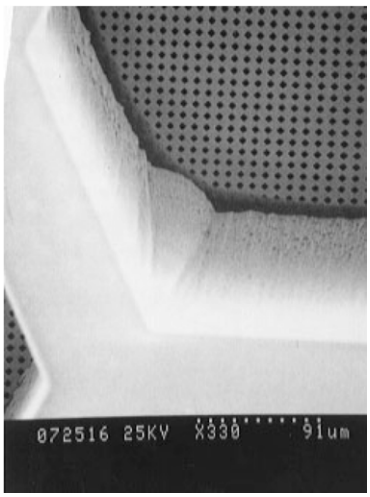

Figure 8. Microporous gas diffusion layer formed in the silicon membrane at the bottom of flow field channels by DRIE. The pore diameter is 4 μm and the silicon membrane thickness is 80 μm.

diameter and 80 μm depth. The integrated GDL provides both high surface area and mechanical support for compression of the MEA to give good electrical contact. The opposite side of the silicon flow field is coated with 1 μm of gold or other corrosion resistant metal to act as a current collector contact to the fuel cell electrode. Fuel cells have been formed either by attaching an existing MEA to the surface having the current collector electrode, or by coating the various layers of the MEA in thin film form to create a monolithic MEA. Efforts are ongoing and moving towards accomplishing this with PBI membranes, with the limiting factors being the approach to attaching the MEA to the electrode formed on the silicon GDL.

5. Conclusion

A MEMS based reformed methanol fuel cell system has been described. The performance of the key components has demonstrated both thermal and chemical compatibility for stable and efficient fuel cell operation by combining a microfluidic methanol fuel processor with a PBI membrane PEM fuel cell. Further integration of fluidic and thermal control systems provides both increased power and energy densities for portable power sources utilizing this approach. Further improvements and scaling of fuel cell stack design will enable both rapid startup operation and higher volumetric energy density for the integrated system.

Acknowledgments

This work was performed under the auspices of the US Department of Energy by the University of California, Lawrence Livermore National Laboratory under Contract No. W-7405-Eng-48.

References

[1] Nowak R 2001 A DARPA perspective on small fuel cells for the military *Solid State Energy Conversion Alliance (SECA) Workshop (Arlington, VA, March 2001)*
[2] Dyer C 2002 Fuel cells for portable applications *J. Power Sources* **106** 31–4
[3] Morse J 2007 Micro-fuel cell power sources *Int. J. Energy Res.* **31** 576–602
[4] Gottesfeld S and Wilson M 2000 Polymer electrolyte fuel cells as potential power sources for portable electronic devices *Energy Storage Systems for Electronics* ed T Osaka and M Dutta (New York: Gordon and Breach Scientific Publishers) pp 487–92
[5] Ren X, Springer T and Gottesfeld S 2000 Water and methanol uptakes in Nafion membranes and membrane effects on direct methanol fuel cell performance *J. Electrochem. Soc.* **147** 92–8
[6] Hirano S, Kim J and Srinivasan S 1997 Solid oxide fuel cells *Electrochim. Acta* **42** 1587–91
[7] Lee S, Chang-Chien A, Cha S, O'Hayre R, Park Y, Saito Y and Prinz F 2002 Design and fabrication of a micro fuel cell array with 'flip-flop' interconnection *J. Power Sources* **112** 410–8
[8] Jankowski A, Morse J, Hayes J and Graff R 2002 Microfabricated thin film fuel cell for portable power requirements *Proc. Materials Research Soc. Symp.* vol 730 pp 93–8
[9] Gold S, Chu K, Lu C, Shannon M and Masel R 2004 Acid loaded porous silicon as a proton exchange membrane for micro-fuel cells *J. Power Sources* **135** 198–203
[10] Wainright J, Savinell R, Liu C and Litt M 2003 Microfabricated fuel cells *Electrochim. Acta* **48** 2869–77
[11] Morse J, Jankowski A, Graff R and Hayes J 2000 Novel proton exchange membrane thin-film fuel cell for microscale energy conversion *J. Vac. Sci. Technol.* A **18** 2003–5
[12] Kelley S, Deluga G and Smyrl W 2000 A miniature methanol/air polymer electrolyte fuel cell *Electrochem. Solid State Lett.* **3** 407–9
[13] Maynard H and Meyers J 2002 Miniature fuel cells for portable power: design considerations and challenges *J. Vac. Sci. Technol.* B **20** 1287–97
[14] Min K, Tanaka S and Esashi M 2006 Fabrication of novel MEMS-based polymer electrolyte fuel cell architectures with catalytic electrodes supported on porous SiO_2 *J. Micromech. Microeng.* **16** 505–11
[15] Ma Y-L, Wainright J S, Litt M H and Savinell R F 2004 Conductivity of PBI membranes for high temperature polymer electrolyte fuel cells *J. Electrochem. Soc.* A **151** 8–16
[16] Peppley B, Amphlett J, Kearns L and Mann R 1999 Methanol-steam reforming on $Cu/ZnO/Al_2O_3$: part 1. The reaction network *Appl. Catal. A: Gen.* **179** 21–9
[17] Holladay J, Jones E, Phelps M and Hu J 2002 Microfuel processor for use in a miniature power supply *J. Power Sources* **108** 21–7
[18] Park H, Malen J, Piggott W, Morse J, Havstad M, Grigoropoulos C, Greif R, Sopchak D and Upadhye R 2006 Methanol steam reformer on a silicon wafer *J. Microelectromech. Syst.* **15** 976–85
[19] Pattekar A V and Kothare M V 2004 A microreactor for hydrogen production in micro fuel cell applications *J. Microelectromech. Syst.* **13** 7–18